Determinant Quantum Monte Carlo simulations of charge density waves in the Holstein model with a double well potential

C. Kvande,[1,2,*] C. Feng,[3] F. Hébert,[4] G. G. Batrouni,[4,5,6,7] and R T. Scalettar[2]

[1]*Physics Department, Kalamazoo College, 1200 Academy Street, Kalamazoo, Michigan, 49006-3295 USA*
[2]*Department of Physics, University of California, Davis, California 95616, USA*
[3]*Center for Computational Quantum Physics, Flatiron Institute, 162 Fifth Avenue, New York, New York 10010*
[4]*Université Côte d'Azur, CNRS, INPHYNI, France*
[5]*Department of Physics, National University of Singapore, 2 Science Drive 3, 117542 Singapore*
[6]*Centre for Quantum Technologies, National University of Singapore; 2 Science Drive 3 Singapore 117542*
[7]*Beijing Computational Science Research Center, Beijing 100193, China*

We use Determinant Quantum Monte Carlo (DQMC) simulations to show that a double well or sombrero potential in the Holstein model may allow for tuning of the critical temperature below which charge density waves (CDWs) form. The original Holstein model is given for reference. We also introduce the background for DQMC and how it compares to standard Monte Carlo techniques. Given some preliminary results in which electron-phonon coupling was not held fixed, we discuss the theoretical basis for further numerical work using a fixed electron-phonon coupling in this model that would allow for comparison with known critical temperatures from the literature. We analyze the available DQMC output, including the structure factor. We demonstrate its use in finite size scaling analysis to find the critical temperature.

I. INTRODUCTION

Broadly, we are interested in modeling phase transitions. In particular, this work is concerned with transitions to the ordered charge density wave (CDW) phase. CDWs are well studied, but there is still more to explore, especially as they relate to superconductivity. In some instances, CDWs are proposed to assist or give rise to unconventional superconductivity, but there are other materials in which they are known to compete with the superconducting phase. Learning more about where they exist and how they interact with other phases is therefore of great interest. [1]

We add to the existing literature by considering a different potential and showing that this may change the critical temperature below which CDWs form. While other investigations have considered the addition of an anharmonic term [2], we specifically consider an anharmonic potential with a double well or sombrero shape. The choice of this potential was inspired by the twofold degeneracy of minima in the original Holstein model potential that allows for particle hole symmetry and hence for charge density waves.

The symmetry of the potential has been proposed to have applications to heavy fermions. Heavy fermions are tied to how conduction electrons in certain compounds interact with an underlying two-level system in that compound. In general, this two level system is magnetic, such that a large external magnetic field should obliterate it, but there are some materials where the heavy fermions survive. Fuse et. al. have argued that a double well potential in the Holstein model may explain the persistence of the heavy fermion behavior even in strong magnetic fields [3]. We are interested in a better understanding of the double well potential in the hopes of revealing more potential connections to observed phenomena.

*Corresponding author: Claire.Kvande19@kzoo.edu

II. MODELS

A. The Original Holstein

The Holstein model, a lattice model that allows for electron - phonon interactions, forms the basis of the project. The standard Holstein Hamiltonian is:

$$\begin{aligned}\hat{H} = &-t\sum_{\langle ij\rangle\sigma}(\hat{c}^{\dagger}_{i\sigma}\hat{c}_{j\sigma}+\hat{c}^{\dagger}_{j\sigma}\hat{c}_{i\sigma})\\ &+\sum_i\frac{\hat{p}_i^2}{2m}+\frac{1}{2}m\omega^2\sum_i\hat{x}_i^2\\ &+\lambda\sum_i\hat{x}_i(\hat{n}_{i\uparrow}+\hat{n}_{i\downarrow})-\mu\sum_i(\hat{n}_{i\uparrow}+\hat{n}_{i\downarrow})\end{aligned}\tag{1}$$

The Holstein model allows electrons to move from some lattice site i to its nearest neighbor at j with tunnelling strength t that is the same in the x and y directions. Throughout this paper, we take t, m, and $\hbar$ equal one. At each of these lattice sites sits a nucleus, represented in the Hamiltonian as a harmonic oscillator. The phonons, or vibrational modes of the lattice, couple to the electrons with coupling strength λ. μ is the chemical potential. The fermionic number operator is defined to be $\hat{n}_{i\sigma} = \hat{c}^{\dagger}_{i\sigma}\hat{c}_{i\sigma}$.

To understand the motivation for studying this model, consider the behavior of the lattice when a single electron is introduced. The nucleus where the electron sits will shift away from its equilibrium position in order to lower the energy of the system. In other words, the nucleus shifts from the minima in the $\hat{n}_{i\uparrow}+\hat{n}_{i\downarrow}=0$ curve, the solid line in Fig. 1, to the minima of the the $\hat{n}_{i\uparrow}+\hat{n}_{i\downarrow}=1$ curve, the dashed line in Fig. 1. If the electron moves to an adjacent site, the original site will return to equilibrium and the new site will adjust instead. In this sense, the electron carries a lattice distortion with it. In addition, overcoming the lowered energy means that the electron now has a higher effective mass.

If we then allow a second electron of opposite spin to be

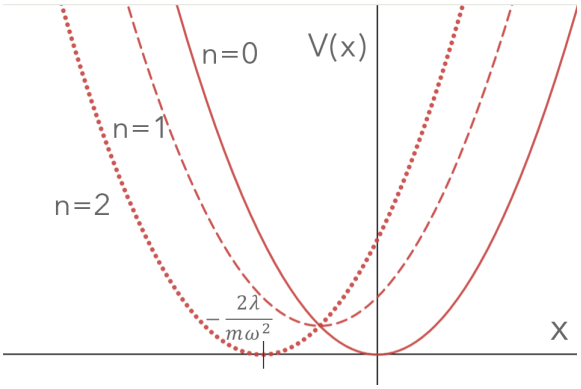

FIG. 1: The three possible $V(x) = \frac{1}{2}m\omega^2x^2 + \lambda x(n_\uparrow + n_\downarrow) - \mu(n_\uparrow + n_\downarrow)$ vs x curves for each of the three values of $n = n_\uparrow + n_\downarrow$. The curves are shown for $\mu = -\frac{\lambda^2}{m\omega^2}$, the value of the chemical potential that corresponds to half filling in the standard Holstein model due to the particle-hole symmetry. The minima of n=1 occurs at the intersection point of the three curves. The n=0 and n=2 minima occur at 0 and $-\frac{2\lambda}{m\omega^2}$, respectively. The minimum energy due to the 'stretching' of the nucleus for electron pairs is equal to energy of the equilibrium configuration, where the nucleus has no electrons, thus showing that we have chosen μ correctly to achieve particle-hole symmetry.

introduced to the system, it will favor the site with the first electron - the electrons are effectively attracted to each other. Looking at Fig. 1, the introduction of the second electron puts the system onto the dotted curve for $\hat{n}_{i\uparrow} + \hat{n}_{i\downarrow} = 2$, where another shift allows it to reach a lower energy than the minima available to a single electron.

When the system is at half filling and below some critical temperature, it becomes an ordered charge density wave pattern of alternating "holes" and "particles" - sites with no electrons and sites with a pair. The equally favorable nature of the electron pairs and the holes can be understood from the two degenerate minima in Fig. 1. We can see this particle-hole symmetry in the potential if we know that the appropriate value of the chemical potential is $\frac{-\lambda^2}{m\omega^2}$. If we take the x-dependant and the chemical potential terms from Eqn. 1 and complete the square, we get:

$$V(x) = \frac{1}{2}m\omega^2(x + \frac{\lambda n}{m\omega^2})^2 - \frac{\lambda^2 n^2}{2m\omega^2} - \mu n \qquad (2)$$

where there are three allowed values of $n = \hat{n}_{i\uparrow} + \hat{n}_{i\downarrow}$. Note that the fermionic number operators can only be 0 or 1, and thus are their own squares. Now substituting our proposed half-filling value of μ and evaluating separately for the three values of n:

$$\begin{aligned} n = 0: &\qquad V(x) = \tfrac{1}{2}m\omega^2x^2 \\ n = 1: &\quad V(x) = \tfrac{1}{2}m\omega^2(x + \tfrac{\lambda}{m\omega^2})^2 + \tfrac{\lambda^2}{2m\omega^2} \\ n = 2: &\qquad V(x) = \tfrac{1}{2}m\omega^2(x + \tfrac{2\lambda}{m\omega^2})^2 \end{aligned} \qquad (3)$$

Comparing these three equations, we can see that the minimum value of $V(x)$ for $n = 0$ and $n = 2$ will be the same, although they occur at different x values. The case of a singly-occupied site, by contrast, will always have higher energy. For the purposes of comparison with our new model, it is important to note that we can shift each of the three curves equally by $\frac{\lambda}{m\omega^2}$, which clearly gives a completely symmetric model: the $n = 1$ curve would have its minima at $x = 0$ and the $n = 0$ and $n = 2$ curves would be reflections of each other with minima at $x = \pm\frac{\lambda}{m\omega^2}$. Future work will use the locations of these minima as a guide for the scaling of the modified Holstein model discussed in the following section.

B. The Double Well Holstein

The existence of these two minima in the traditional Holstein model motivates the choice of potential in the modified version. Thus the model we are interested in uses a double-well potential for a nucleus even before electrons are introduced, making the new Hamiltonian:

$$\begin{aligned} \hat{H} = &-t\sum_{\langle ij\rangle\sigma}(\hat{c}^\dagger_{i\sigma}\hat{c}_{j\sigma} + \hat{c}^\dagger_{j\sigma}\hat{c}_{i\sigma}) \\ &+ \sum_i \frac{\hat{p}_i^2}{2m} + A\sum_i \hat{x}_i^2 + B\sum_i \hat{x}_i^4 \\ &+ \lambda\sum_i \hat{x}_i(\hat{n}_{i\uparrow} + \hat{n}_{i\downarrow} - 1) - \mu\sum_i(\hat{n}_{i\uparrow} + \hat{n}_{i\downarrow}) \end{aligned} \qquad (4)$$

The new parameters, $A = -\frac{1}{2}m\omega^2$ and B define a double well potential, as shown in Fig. 2. To ensure the double well shape, we always choose A negative and B positive. Note that the presence of this potential fundamentally changes the minima found in the original Holstein model. Here, we hope that the new model will be more tunable than the original model, yet with a similar two-choice structure to encourage charge density wave formation.

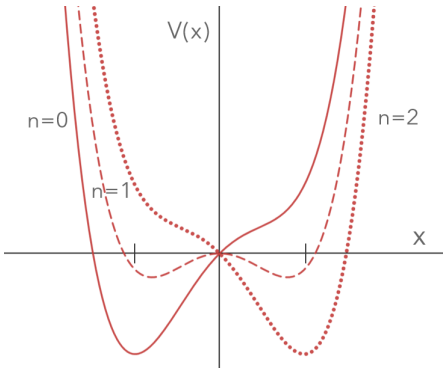

FIG. 2: The three possible $V(x) = Ax^2 + Bx^4 + \lambda x(\hat{n}_{i\uparrow} + \hat{n}_{i\downarrow} - 1) - \mu(\hat{n}_{i\uparrow} + \hat{n}_{i\downarrow})$ vs x curves for each of the three values of $n = n_\uparrow + n_\downarrow$. All are shown for the particle-hole symmetric case of $\mu = 0$. Future work will align the global minima in this model with where they would be in the original model.

It is important to point out that we could re-write the first term on the final line of Eqn. 4 to be in terms of the phonon

creation and destruction operators, a_i and $a_i^\dagger$, so that it becomes $g\sum_{i\sigma}(a_i^\dagger + a_i)n_{i\sigma}$. The new constant is related to the old electron-phonon coupling as $g = \lambda/\sqrt{2\omega}$. For the work discussed in this paper, we choose $g = 1$, which means λ must vary with ω as we change the value of the coefficient A. This relationship will change in future work so that λ and A are decoupled: A will no longer depend on λ.

The additional -1 in the electron-phonon coupling term on the third line ensures that the new model is still particle-hole symmetric at $\mu = 0$. As a loose proof, we can see that the general partition function in the single site limit has the form:

$$Z = \sum_{\hat{n}_{i\uparrow}=0}^{1}\sum_{\hat{n}_{i\downarrow}=0}^{1}\int dx e^{-\beta[V(x)]} \tag{5}$$

where,

$$V(x) = Ax^2 + Bx^4 + \lambda x(\hat{n}_{i\uparrow} + \hat{n}_{i\downarrow} - 1) - \mu(\hat{n}_{i\uparrow} + \hat{n}_{i\downarrow}). \tag{6}$$

To show that $\mu = 0$ is the appropriate value for half filling, we solve

$$\langle n_\uparrow\rangle = Z^{-1}\sum_{\hat{n}_{i\uparrow}=0}^{1}\sum_{\hat{n}_{i\downarrow}=0}^{1}\int dx n_\uparrow e^{-\beta V(x)} = \frac{1}{2} \tag{7}$$

The integral is only non-zero when $n_\uparrow = 1$. If we introduce the notation $I(n_\uparrow, n_\downarrow)$ to denote the integral for a specific choice of number operators, we can re-write Eqn. 7 as:

$$\langle n_\uparrow\rangle = \frac{I(1,0) + I(1,1)}{I(0,0) + 2I(1,0) + I(1,1)} = \frac{1}{2} \tag{8}$$

where the denominator comes from our previous definition of the partition function and the understanding that $I(1,0) = I(0,1)$. Rearranging this easily shows that the condition for this equation to hold is that $I(0,0) = I(1,1)$, which can only be true when $\mu = 0$; otherwise, one of the two curves would be shifted to a lower energy relative to the other. Referring back to Eqn. 5, we see that, when $\mu = 0$, the curves of $V(x)$ as a function of x are reflections of each other in the y axis, as shown in Fig. 2.

III. METHODS

The main method of analysis for this study is Determinant Quantum Monte Carlo (DQMC). We used an exact diagonalization code to check the DQMC in the single-site limit ($t = 0$), but beyond this the calculations become unreasonable.

I also checked the DQMC measurements against results from Langevin calculations. By contrast to the DQMC methods that will be discussed in the second portion of this section, Langevin calculations scale with the number of sites. However, there is an additional step size error associated with the implementation of the random force that serves as the 'dynamics' in Langevin simulations [4].

A. Classical Monte Carlo

Classical Monte Carlo methods allow systems of classical observables, like the magnetization of the Ising model, to be simulated accurately by proposing a change at each site in the system and accepting them if a random number falls below a ratio of the old to new Boltzmann distribution - that is, the change in energy that would result from the move determines the cutoff. By performing many such proposals and averaging measurements over many iterations, classical Monte Carlo has powerful predictive potential for systems from phase transitions to protein folding.

There are many versions of Monte Carlo, perhaps the most widely known being the Metropolis algorithm, but all share two key features. The first requirement is that the system be ergodic : each state in the system must have a non zero probability, and be accessible from any other state, even if not directly. [5]

The second, somewhat more complicated condition, is detailed balance. Detailed balance requires that there be a steady-state solution where the probability of entering some state is the same as the probability of leaving. Mathematically, we first define the transition matrix T, where each element $T_{ij} = T(i \to j)$ is the probability that the system in state i will transform directly into state j. Therefore, we require that the matrix be stochastic: $T_{ij} \geq 0$ and $\sum_j T_{ij} = 1$. In other words, there are no negative probabilities, and the probability of being in a given state i must be normalized. This fits with our previous ergodicity requirement, and can also be used to show the condition of detailed balance, which is written as:

$$p(i)T(i \to j) = p(j)T(j \to i) \tag{9}$$

Using this representation of detailed balance, we can show that $p(i)$, the probability distribution, is the eigenvector of T with eigenvalue 1 [5]:

$$\begin{aligned}\sum_i p(i)T(i \to j) &= \sum_i p(j)T(j \to i) \\ &= p(j)\sum_i T(j \to i) = p(j)\end{aligned} \tag{10}$$

Since stochastic matrices have a maximum eigenvalue of one, we known we have found the eigenvector with the largest eigenvalue. Furthermore, there is a theorem that states that applying a matrix many times to a vector transforms that vector to point in the direction of the eigenvector corresponding to the maximum eigenvalue. Thus, we have shown that the process of Monte Carlo, in which we apply the transition matrix repeatedly to some initial state, will always converge to the correct probability distribution in the limit of a large enough number of sweeps.

Sometimes, however, the number of sweeps needed for the system to reach equilibrium is prohibitively large. Several things may be done to improve the convergence time: first, we generally try to choose a configuration close to the equilibrium solution, if it is known. In the modified Holstein model, we chose to initialize the phonon fields in a pattern of alternating positive and negative displacements about equilibrium - a good starting point for a charge density wave.

Additionally, we incorporate global moves into the algorithm. This is especially important in systems such as those being considered here, that have two possible minima. If the system were allowed to run indefinitely, the values of the phonon fields would eventually switch from one well to the other, but in the limit of realistic computation times, it is more likely that the system gets stuck around where it started. Thus, we implement global moves, wherein the proposed move is a "flip" from one well to another. The tuning of these global moves, which depends intimately on the locations of the two minima, is important to the feasibility of the study.

B. Determinant Quantum Monte Carlo

Quantum Monte Carlo makes use of Feynman's path integral formalism to recast a d-dimensional quantum problem as a d+1-dimensional classical problem. The quantum problem of interest has a trace as its partition function:

$$Z = Tre^{-\beta\hat{H}}. \tag{11}$$

The new dimension to be added is the imaginary time axis. The imaginary time dimension is determined by the inverse temperature, β, by dividing it into small intervals $\Delta\tau$ such that $\beta = L\Delta\tau$. This allows for use of the Trotter approximation, by which we decompose the Hamiltonian into several distinct terms despite the fact that they do not commute. The error for this approximation goes as $t\lambda(\Delta\tau)^2$, so we make a point to choose $\Delta\tau$ small [6] [7]. In the implementation for this work, $\Delta\tau$ is always $1/16$ and $t = 1$. With the choice of $\lambda = 2$ in future work, the error for the approximation is $1/128$.

In splitting up the Hamiltonian, we consider the position and momentum operators as distinct from each other and from the portions containing fermionic operators. Thus the trace to be done becomes:

$$e^{-\beta\hat{H}} \approx (e^{-\Delta\tau\hat{H}_x}e^{-\Delta\tau\hat{H}_p}e^{-\Delta\tau\hat{H}_{el}})^L \tag{12}$$

where $\hat{H}_x$ has the terms with only position operators, $\hat{H}_p$ is the momentum operator term, and $\hat{H}_{el}$ has any terms with fermionic operators, including the electron-phonon coupling.

We first consider the phonon portion, which we treat with the Feynman path integral formalism [5] [6] . To move from position operators to their eigenvalues, we first add a complete set of position states between each pair of exponentials, as below:

$$\begin{aligned}
&\mathrm{Tr}(e^{-\Delta\tau\frac{\hat{p}^2}{2m}}e^{-\Delta\tau(-\frac{1}{2}m\omega^2\hat{x}^2+B\hat{x}^4)})^L \\
&= \int dx\langle x_1|[e^{-\Delta\tau\frac{\hat{p}^2}{2m}}e^{-\Delta\tau(-\frac{1}{2}m\omega^2\hat{x}^2+B\hat{x}^4)}]^L|x_1\rangle \\
&= \int dx_1\cdots dx_L e^{\frac{1}{2}m\omega^2\Delta\tau\sum_{l=1}^{L}x_l^2 - B\Delta\tau\sum_{l=1}^{L}x_l^4} \\
&\langle x_1|e^{-\Delta\tau\frac{\hat{p}^2}{2m}}|x_L\rangle\langle x_L|e^{-\Delta\tau\frac{\hat{p}^2}{2m}}|x_{L-1}\rangle\cdots\langle x_2|e^{-\Delta\tau\frac{\hat{p}^2}{2m}}|x_1\rangle
\end{aligned} \tag{13}$$

This is allowed because

$$I = \int dx|x\rangle\langle x| \tag{14}$$

so we are simply multiplying by the identity in several places. However, we still have momentum operators acting on our position states, so we now add a complete set of momentum states, which for any such exponential in Eqn. 13 goes as:

$$\begin{aligned}
&\int dp\langle x_{l+1}|e^{-\Delta\tau\frac{\hat{p}^2}{2m}}|p\rangle\langle p|x_l\rangle \\
=&\int dpe^{-\Delta\tau\frac{p^2}{2m}}e^{-ipx_{l+1}}e^{ipx_l} \\
=&\int dpe^{-\Delta\tau\frac{1}{2m}[p^2+i2pm\frac{(x_{l+1}-x_l)}{\Delta\tau}]} \\
=&\sqrt{\frac{2m\pi}{\Delta\tau}}e^{-\frac{1}{2}m(\frac{x_{l+1}-x_l}{\Delta\tau})^2}
\end{aligned} \tag{15}$$

All together this becomes:

$$Z_{ph} = \int dx_1\cdots dx_L e^{-\Delta\tau S_{ph}} \tag{16}$$

with the classical action given by:

$$\begin{aligned}
&S_{ph} = \\
&-\frac{1}{2}m\omega^2\sum_{l=1}^{L}x_l^2 + B\sum_{l=1}^{L}x_l^4 + \frac{1}{2}m\sum_{l=1}^{L}\Big(\frac{x_{l+1}-x_l}{\Delta\tau}\Big)^2
\end{aligned} \tag{17}$$

We consider the electron contribution slightly differently; although this can also be done in the path integral formalism by way of Grassman coherent states [4], what follows is a simplified version [8] [7]. Consider the electron contribution at each time step τ:

$$\hat{H}_{el}(\tau) = \begin{pmatrix}\hat{c}^\dagger_{1\downarrow}...\hat{c}^\dagger_{N\downarrow}\end{pmatrix}\kappa\begin{pmatrix}\hat{c}_{1\downarrow}\\ \vdots \\ \hat{c}_{N\downarrow}\end{pmatrix},$$

$$\kappa = \begin{pmatrix}-\mu-\lambda x_1(\tau) & -t & 0 \\ -t & -\mu-\lambda x_2(\tau) & -t \\ \ddots & \ddots & \ddots \\ 0 & -t & -\mu-\lambda x_N(\tau)\end{pmatrix} \tag{18}$$

where we have chosen to show only the spin-down electrons, although there is no difference with the spin up.

The quantum partition function is a trace over a 4^N dimensional Hilbert space, which can be done easily if it is quadratic in the fermion operators [7], thanks to the identity:

$$Z = \mathrm{Tr}e^{-\beta\hat{H}} = \det[I + e^{-\beta h}] \tag{19}$$

where h is an NxN matrix of numbers, and I is the identity matrix. This identity also extends to a set of such operators $\hat{H}(l)$ as

$$\begin{aligned}
Z &= \mathrm{Tr}[e^{-\Delta\tau\hat{H}(1)}...e^{-\Delta\tau\hat{H}(L)}] \\
&= \det[I + e^{-\Delta\tau h(1)}...e^{-\Delta\tau h(L)}]
\end{aligned} \tag{20}$$

as long as they are all also quadratic in the fermion creation and destruction operators.

To make use of this identity in order to simplify the treatment of the fermionic portion of the problem, we define the matrix M as:

$$M = I + \exp\begin{pmatrix} -\mu - \lambda x_1(1) & -t & 0 \\ -t & \ddots & -t \\ 0 & -t & -\mu - \lambda x_N(1) \end{pmatrix}$$

$$\cdots \exp\begin{pmatrix} -\mu - \lambda x_1(L) & -t & 0 \\ -t & \ddots & -t \\ 0 & -t & -\mu - \lambda x_N(L) \end{pmatrix} \quad (21)$$

where each exponential has a matrix of information for all sites from 1 to N, and there are L total exponentials being multiplied together, one for each imaginary time slice. We can now rewrite the fermionic trace as a determinant of M.

Finally, combining this with the phonon terms, we can rewrite our original partition function as:

$$\begin{aligned} Z &= \mathrm{Tr} e^{-\beta \hat{H}} \\ &= \int \Pi_i \, \Pi_\tau \, dx_i(\tau) \, e^{-\Delta\tau S_{ph}} \det M_\uparrow \det M_\downarrow \end{aligned} \quad (22)$$

Since, as previously noted, the up and down spins are treated the same - there are no direct electron-electron interactions to require differentiation between the two- the two determinants are identical and can be replaced by $(\det M)^2$. This avoids one of the potential limitations associated with DQMC, the fermionic sign problem, which, while it does not arise in the model considered here, has devastating consequences in other systems. Because of the presence of a negative sign difference in how the spin up and down electrons couple, there are some systems (such as the Hubbard model away from half filling) where the determinant, and hence the probabilities, can become negative [6] [8]. This is unphysical, and prohibits the use of the method for such systems. In the Holstein model, luckily, the two spins are treated identically, and thus no difference of sign arises.

Another notable feature of this algorithm is that the action is non-local, which means that the CPU time needed for any calculation goes as the cube of the number of sites.

IV. RESULTS AND DISCUSSION

Since we are looking for charge density waves, the observables of interest are the density-density correlation function and its Fourier transform, the structure factor [9]. The density-density correlation function tracks how strongly related any given site is to any other. In perfect charge density wave order, every site is anti-correlated to the density of its nearest-neighbors and highly correlated with its next-nearest neighbors, leading to a periodic fluctuation in the density-density correlation function. In real space, it looks like Fig. 3, with

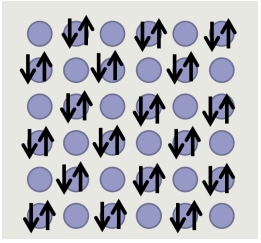

FIG. 3: Perfect CDW order in real space, where pairs of arrows are pairs of electrons on a nucleus and the circles are holes. The lattice is exactly half filled. This configuration corresponds to a peak in the structure factor at momentum (π, π).

alternating pairs of electrons and holes on a lattice of nuclei. This makes it an excellent quantity to Fourier transform: in ideal CDW order, we expect a strong peak at momentum (π, π) in the structure factor, which is given by:

$$S_{cdw} = \sum_i \langle n_i n_{i+j} \rangle (-1)^j. \quad (23)$$

where i labels some site and $j = j_x + j_y$ is the distance to the neighbor at $i + j$ that it is compared to. The structure factor is plotted in Fig. 4.

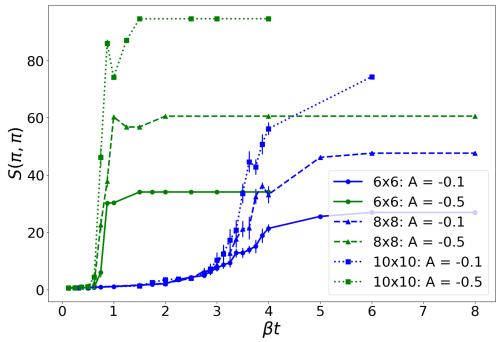

FIG. 4: The structure factor at (π, π) as a function of β for $A = -0.1$ (blue) and $A = -0.5$ (green). Each value of A is shown for three different lattice sizes: L=6 (solid line, circles), L=8 (dashed, triangles), L=10 (dotted, squares). All data is done with $B = 0.01$, $\mu = 0$, and $g = 1$. At low values of the inverse temperature, the system does not depend on lattice size, but the different lattice sizes begin to diverge at $\beta_{critical}$.

In order to determine where exactly symmetry breaking takes place, we make use of finite scaling effects. In a high-temperature system, the charge density is disordered and the correlation length is very small. Thus at high temperatures, we expect all lattice sizes to behave the same. As the temperature is lowered, the correlation length increases as the system approaches an overall ordered phase, and eventually the correlation length and the scale of the system will be the same.

Clearly this will happen at different points for systems of different sizes, hence the disagreement of different L at the lower temperatures (higher beta) in Fig 4.

The point where the different lattice sizes begin to diverge is the critical temperature. In the case of $A = -0.1$ (blue), we can see from Fig. 4 that the intersection is around $\beta = 3$. For a better analysis of where the critical temperature is, we make use of the finite size scaling to rescale the data such that all lattice sizes will intersect at the critical temperature. The key to this rescaling is the fact that this model falls under the same universality class as the 2D Ising model, which means the scaling uses the critical exponents of the 2D Ising model [6]. Multiplying every point in Fig. 4 by its lattice size raised to $\frac{-7}{4}$ power results in Fig. 5. Here, we can see that the three curves intersect at about $\beta = 3.5$.

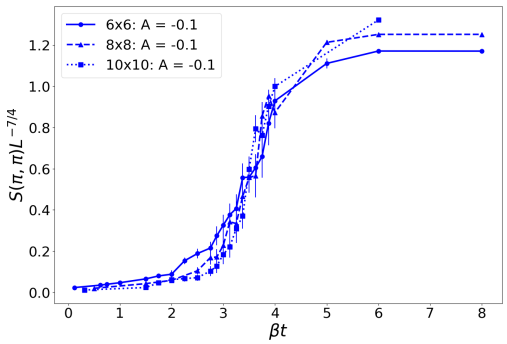

FIG. 5: The structure factor for $A = -0.1$ is shown for three different lattice sizes: L=6 (solid line, circles), L=8 (dashed, triangles), L=10 (dotted, squares). All data is done with $B = 0.01$, $\mu = 0$, and $g = 1$. In this plot, the structure factor is scaled by $L^{-7/4}$, as for all systems in the 2D Ising criticality class, so that finite size scaling effects allow determination of the critical temperature based on the intersection of the three curves.

Further observables of interest include the energy, the density, and the double occupancy. The density and double occupancy in particular are useful for quantifying how well formed the charge density wave is. If the CDW order is perfect, we expect density of one and double occupancy of a half. In Fig. 6, we can see that this order is not quite perfect, especially for $A = -0.1$.

The energy, particularly when broken down into electronic and phontonic portions and potential and kinetic, can help us understand how the system behaves around the critical point. In Fig. 7, we show the electronic kinetic energy, which has an interesting peak just before the proposed critical temperature. If this feature survives after further runs, it may be a key to understanding the charge density wave formation.

V. CONCLUSIONS AND FURTHER WORK

Through this work, we were able to show that changing the parameter A in a modified Holstein with a double-well

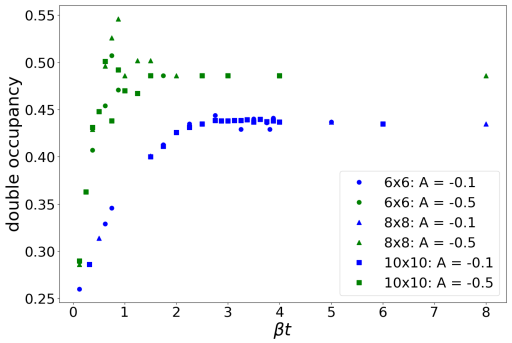

FIG. 6: The double occupancy as a function of β is shown for $A = -0.1$ (blue) and $A = -0.5$ (green). Each value of A is shown for three different lattice sizes: L=6 (solid line, circles), L=8 (dashed, triangles), L=10 (dotted, squares). All data is done with $B = 0.01$, $\mu = 0$, and $g = 1$. In perfect CDW order, we expect the double occupancy to be 0.5.

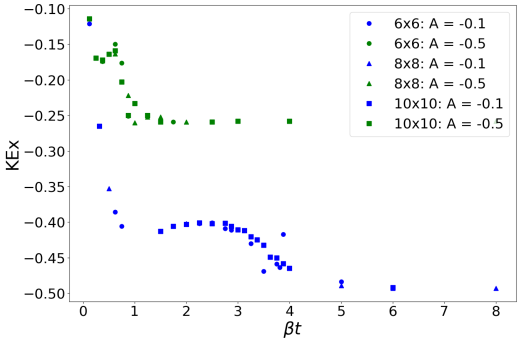

FIG. 7: The electronic kinetic energy in the x direction as a function of β is shown for $A = -0.1$ (blue) and $A = -0.5$ (green). Each value of A is shown for three different lattice sizes: L=6 (solid line, circles), L=8 (dashed, triangles), L=10 (dotted, squares). All data is done with $B = 0.01$, $\mu = 0$, and $g = 1$. The y direction is identical, since the hopping strength is uniform.

potential allows for tuning of the critical temperature below which charge density waves form.

There is a caveat to this success: since changing A is tied to changing ω and therefore λ, there is a chance that the observed changes in the critical temperature are partly due to the increases in the electron-phonon coupling, rather than A alone. This would imply a trivial scaling of the model. However, even this trivial scaling cannot completely account for the increase in T_c observed in this work: the original Holstein model does not simply increase with lambda, but instead reaches a peak at a specific value of lambda. For a square lattice and the conventional Holstein model, T_c reaches a maximum value of about 0.24, compared to $T_c \approx 0.28$ found in this work for $A = -0.1$ [11]. To eliminate the portion of T_c scaling that is a result of the electron-phonon coupling, new

runs will drop the dependence on ω in the model, simply leaving A and λ as separate parameters.

To allow for a fair comparison between the modified model and the original Holstein model, we will fix the value of λx_0 at which the minima in the energy occur, so that Fig. 1 and Fig. 2 are on the same scale. In practice, this means picking a value of x_0 based on previous studies, then choosing A and B such that the minima in the sombrero occur at the same place. We will likely choose $\lambda = 2$ and $\omega = 1$ so that $x_0 = \frac{\lambda}{\omega^2} = 2$ in the conventional Holstein model as the basis of comparison. In the version with a double-well potential, we can then choose a value of B such that A must be:

$$A = \frac{\lambda - 4Bx_0^3}{2x_0} \tag{24}$$

If desired, we may also choose to vary A away from this "fair" comparison, but establishing this baseline will make sure any changes in T_c are not due to a difference in the electron-phonon coupling.

The analysis and methods for this slight modification to the model will remain the same: we will still use Determinant Quantum Monte Carlo and are still interested in using the structure factor to establish the presence of charge density waves.

There is also potential for interesting physics in the system's behavior away from half filling, i.e. $\mu \neq 0$. We hypothesize that the intrinsic double-well shape of the phonon potential will allow charge density waves to form and be stabilized even without perfect half filling.

Bibliography

[1] X. Zhu, J. Guo, J. Zhang and E. W. Plummer, "Misconceptions associated with the origin of charge density waves," *Advances in Physics* **2**, 622 (2017).

[2] G. Paleari, F. Hebert, B. Cohen-Stead, K. Barros, R.T. Scalettar and G.G. Batrouni, "Quantum Monte Carlo study of an anharmonic Holstein model," *Physical Review B* **103**, 195117 (2021).

[3] T. Fuse, Y. Ono, and T. Hotta, "Heavy-Electron Formation and Polaron–Bipolaron Transition in the Anharmonic Holstein Model," *Journal of the Physical Society of Japan* **81**, 044701 (2012).

[4] G. Batrouni, "Determinant and Langevin Quantum MC," presentation and slides.

[5] M. Creutz and B. Freedman, "A Statistical Approach to Quantum Mechanics," *Annals of Physics* **132**, 427 (1981).

[6] R. T. Scalettar, "World Line Quantum Monte Carlo."

[7] C. Chang, S. Gogolenko, J. Perez, Z. Bai, and R. T. Scalettar, "Recent advances in determinant quantum Monte Carlo," *Philosophical Magazine* **95**, 1260 (2015).

[8] R. T. Scalettar, "Computational quantum magnetism: Determinant Quantum Monte Carlo," *Lecture notes for Boulder Summer School* (2003).

[9] Y.-X. Zhang, W.-T. Chiu, N.C. Costa, G.G. Batrouni, and R.T. Scalettar, "Charge Order in the Holstein Model on a Honeycomb Lattice," *Phys. Rev. Lett.* **122**, 077601 (2019).

[10] J. Kondo, "Localized atomic states in metals," *Physica B+C* **84**, 40 (1976).

[11] B. Cohen-Stead, K. Barros, ZY Meng, C. Chen, R.T. Scalettar, and G.G. Batrouni, "Langevin sumulations of the half-filled cubic Holstein model," *Physical Review B* **102**, 161108 (2020).